Binding of IP_3 and Adenophostin A to the N-terminal of the IP_3 Receptor: Thermodynamic Analysis Using Fluorescence Polarization with a Novel IP_3 Receptor Ligand

Data Supplement

A

Primer	Sequence
P1	CGGGATCCATGTCTGACAAAATGTCTAGT
P2	CGCGCTCGAGTCACTTTCGGTTGTTGTGGA
P3	CGGGATCCATGAAATGGAGTAACAAAG
P4	ATTACTTGGCAGCAGAGGTAGACCCTGACTTTGAGGAAGAATGCCTGGAGTTTCAGCCCTCAGTGGACCCTGATCAGG
P5	GATCAGGGTCCACTGAGGGCTGAAACTCCAGGCATTCTTCCTCAAAGTCAGGGTCTACCTCTGCTGCCAAGTAATGC

B

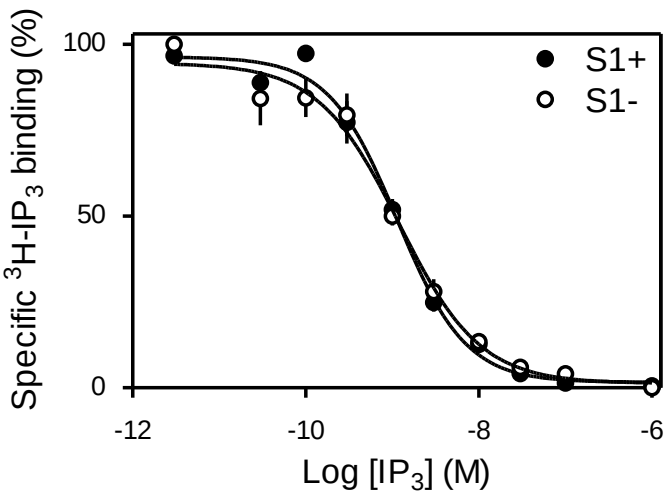

Supplemental Fig. 1. Preparation of plasmids encoding NT and IBC. Primers used to generate the plasmids encoding the IBC and NT (A). Specific ^{3}H-IP_3 binding (0.25 nM) in TEM to the IBC with ($S1^+$) or without ($S1^-$) the S1 splice region (B). Results are means $\pm$ S.E.M., $n \geq 4$.

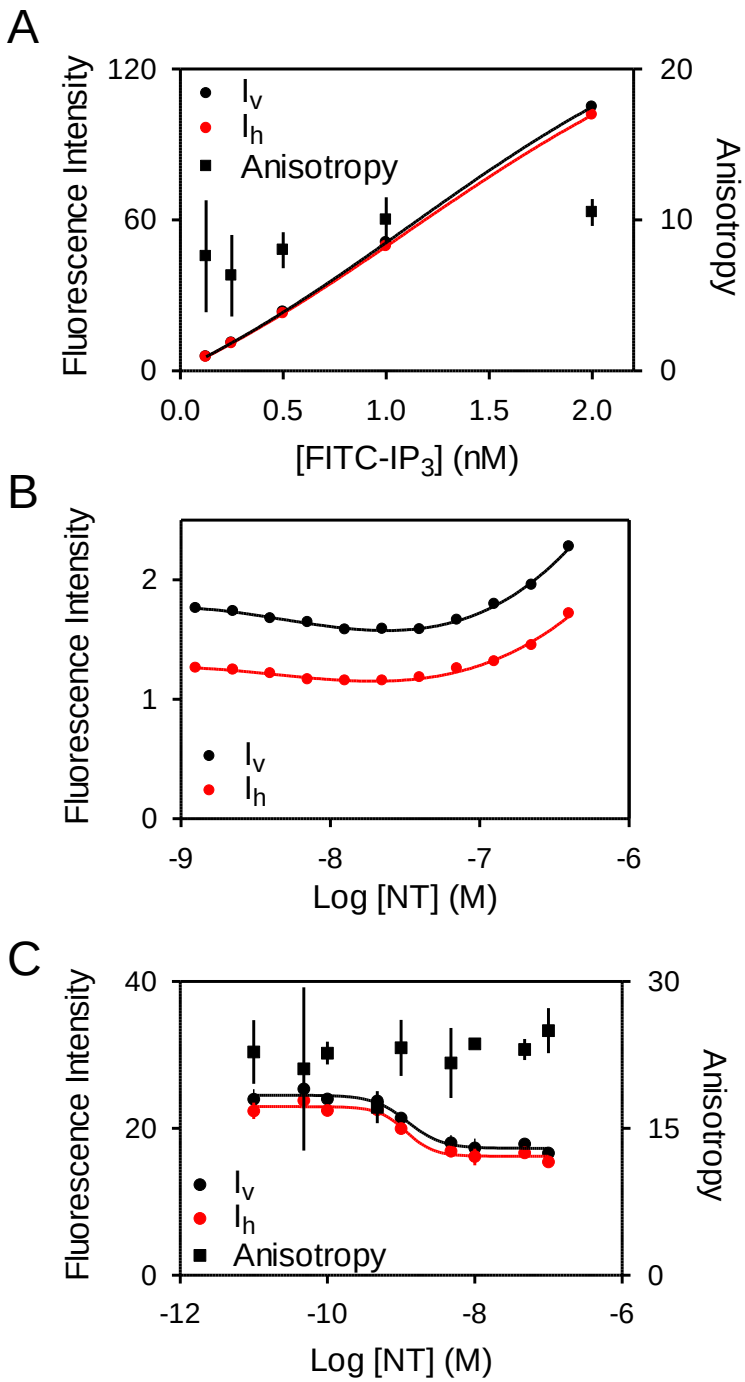

Supplemental Fig. 2. Optimizing signal-noise for FP assay of ligand binding to IP_3R in CLM. Emitted fluorescence in the vertical (I_v) and horizontal (I_h) planes and anisotropy (*A*) were measured for the indicated concentrations of free FITC-IP_3 (A). Across a 16-fold range of FITC-IP_3 concentration, there is a linear relationship between fluorescence (I_v and I_h) and no significant difference in anisotropy. The results demonstrate that with an even lower concentration of FITC-IP_3 (0.125 nM) than used in our assays (0.5 nM), background fluorescence does not perturb measurements of *A*. Fluorescence in the vertical (I_v) and horizontal (I_h) planes from the indicated concentrations of NT in the absence of FITC-IP_3 (B). These results demonstrate that at the highest protein concentrations used in saturation binding experiments (Fig. 3A), the contribution from background fluorescence is <15% of the total signal (which derives largely from bound FITC-IP_3). Because this protein fluorescence is unrelated to FITC-IP_3, all measurements were corrected for the small background signal by measuring I_v and I_h from a parallel sample of protein without FITC-IP_3. The effects of protein (NT at the indicated concentrations) on the emitted fluorescence (I_v and I_h) from free FITC-IP_3 (0.5 nM) was measured in the presence of 10 µM IP_3 (to ensure that FITC-IP_3 is displaced from all IP_3-binding sites) (C). Because quenching was the same in all planes, *A* was unaffected by increasing [NT]. This quenching effect does not therefore affect experimental measurements of *A*; no correction was therefore required.

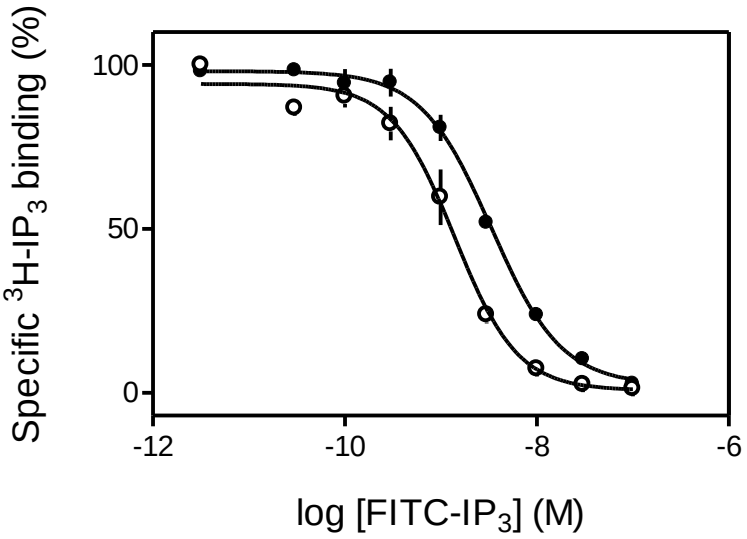

Supplemental Fig. 3. Specific binding of ^{3}H-IP$_3$ to the NT (○) and full-length IP$_3$R (●) in TEM in the presence of the indicated concentrations of FITC-IP$_3$. The ^{3}H-IP$_3$ concentrations used were 0.75 nM and 1 nM for the NT and full-length IP$_3$R, respectively. Results are means ± S.E.M, n = 3.

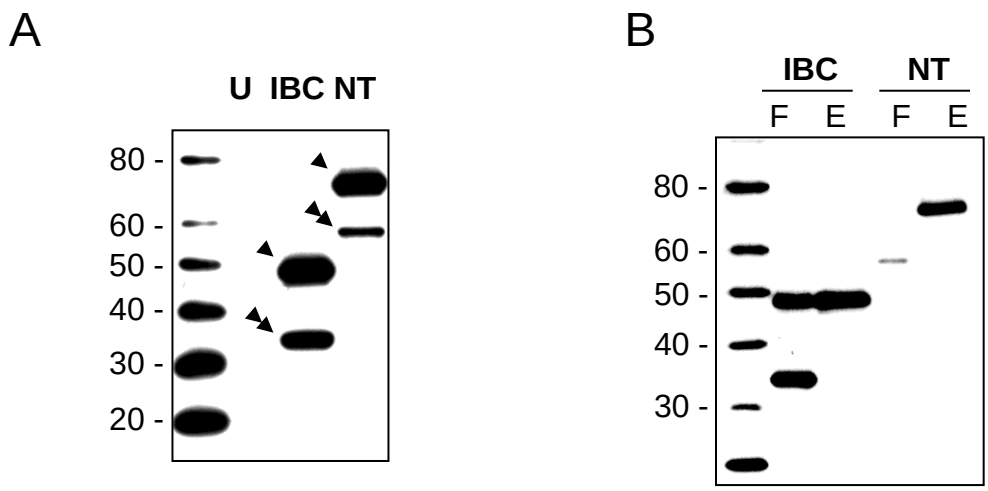

Supplemental Fig. 4. **Expression of N-terminal fragments of IP_3R1 and elution from heparin columns.** Lanes were loaded with lysate (5 μg of protein) from untransformed bacteria (U) and bacteria expressing N-terminally His_6-tagged IBC and NT fragments of IP_3R1. Bands were detected with anti-His_6 antibody. Arrows denote the bands corresponding to the full-length constructs with the expected mass; double arrows show bands of lower molecular mass, which may be truncated versions or degradation products (A). Full-length IP_3R and its N-terminal fragments are retained on a heparin-agarose column in the presence of 0.25 M NaCl and are then eluted with 0.5 M NaCl (not shown). Bacterial lysates of IBC and NT in 0.25 M NaCl were passed over heparin-agarose columns and samples were collected from the flow-through fraction (labelled F) and after elution (labelled E) with 0.5 M NaCl. Fragments were visualised by immunoblotting with an anti-His_6 antibody. Whereas bands with the mobilities expected of the full-length fragments were retained on the heparin column, smaller fragments were collected entirely in the flow-through fraction). We conclude that the lower molecular mass proteins are unlikely to bind IP_3 because they do not bind to heparin (B). Representative blots of at least 3 independent experiments are shown. Molecular weight markers are shown on the left of each blot.

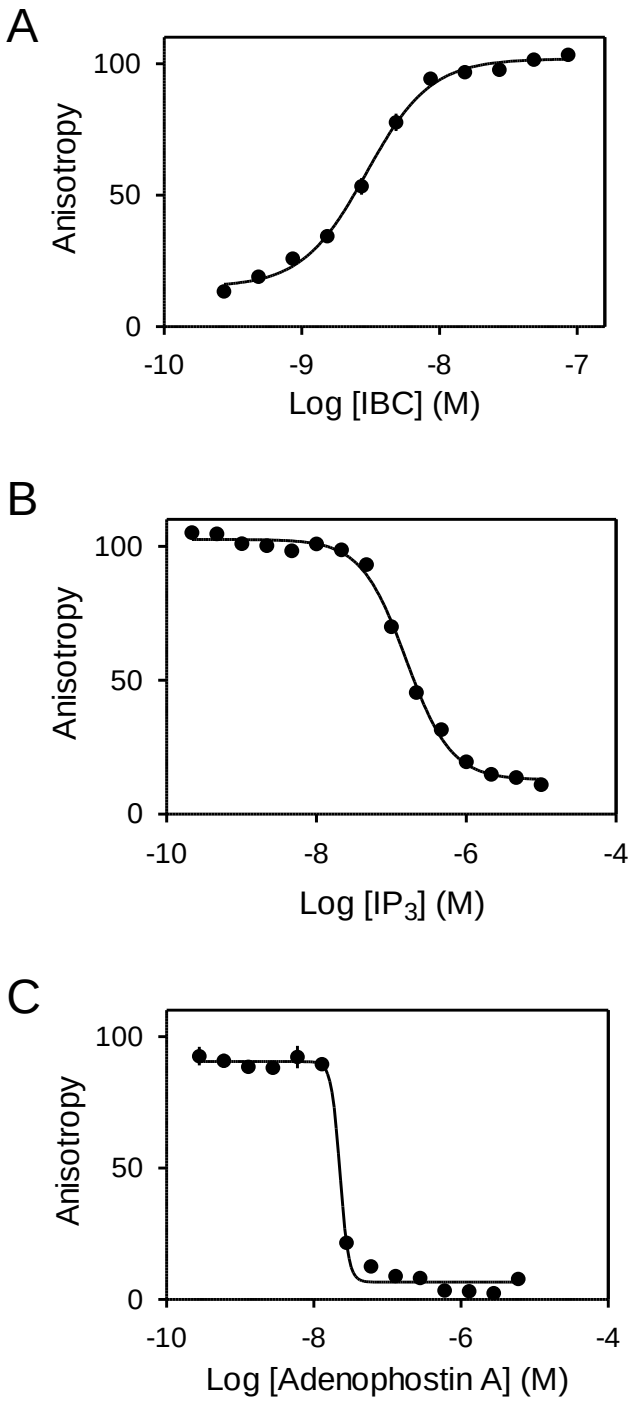

Supplemental Fig. 5. FITC-IP_3, IP_3 and adenophostin A binding to the IBC analysed by FP in CLM. FP experiment at 4ºC using 0.5 nM FITC-IP_3 and showing corrected *A* as a function of increasing concentrations of the IBC (A). FP competition binding assay with FITC-IP_3 (0.5 nM), IBC (15 nM) and the indicated concentrations of IP_3 (B) or adenophostin A (C). Results are means ± S.E.M., n = 3. Equivalent analyses with the NT are shown in Fig. 3.

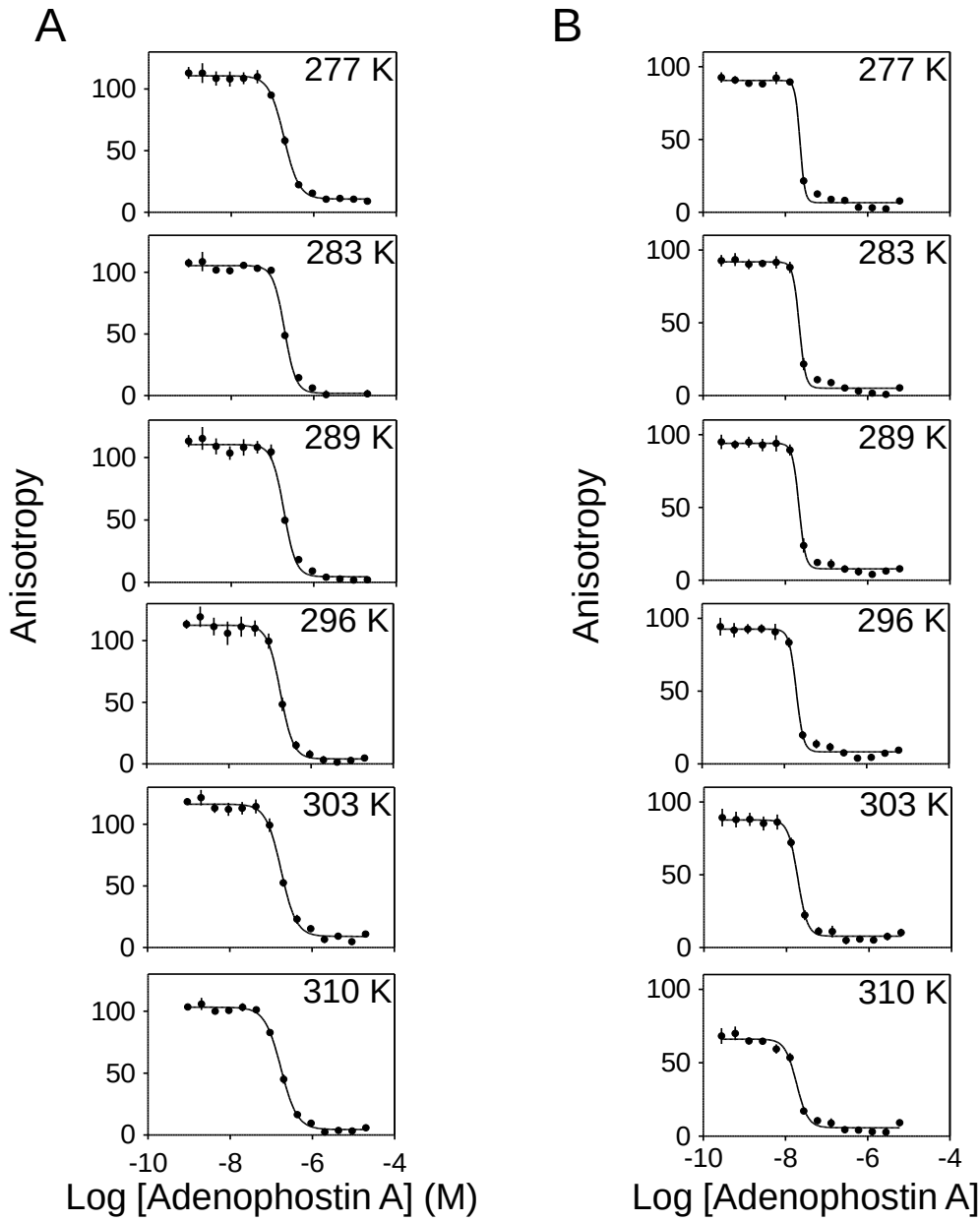

Supplemental Fig. 6. Effects of temperature on adenophostin A binding in CLM. FP competition binding assays with FITC-IP_3 (0.5 nM) and adenophostin A and the NT (A, 80 nM) or IBC (B, 15 nM) at the indicated temperatures. Results are means $\pm$ S.E.M., n = 3. Similar analyses for IP_3 are shown in Fig. 4, and the results are summarized in Table 4.

Supplemental Table 1
Thermodynamics of IP_3 and adenophostin A binding to the NT and IBC analysed without assuming that ΔC is zero.
From the effects of temperature on IP_3 and adenophostin A binding to the IBC and NT in CLM (Table 4, Fig. 4 and Supplemental Fig. 6), ΔG (equation 10) was determined and thereby ΔH, ΔC and ΔS (equation 11). -TΔS is also shown for 296 K. Results are means ± S.E.M., n = 3.

		ΔG kJ /mol (296 K)	ΔH kJ/mol (296 K)	ΔC J/mol.K	ΔS J/mol.K (296 K)	-TΔS kJ/mol (296 K)
IP_3	NT	-37.1 ± 0.2	-35.9 ± 1.4	319 ± 65	4.4 ± 4.6	-1.3 ± 1.4
	IBC	-43.2 ± 0.2	-37.8 ± 0.2	-425 ± 72	18.1 ± 0.4	-5.4 ± 0.1
Adenophostin A	NT	-43.5 ± 0.03	-30.9 ± 1.5	170 ± 196	42.6 ± 5.0	-12.6 ± 1.5
	IBC	-49.4 ± 0.3	-18.7 ± 1.6	1026 ± 206	103.4 ± 5.2	-30.6 ± 1.5